This is the Pre-Published Version.

C. Xiong, Z. Wang, Y. Huang, F. Shi, X. Huang (2022) *Smart Building Fire Hazard Evaluation by Attenuation of Alarm Sound Field*, **Journal of Building Engineering**, 104264. https://doi.org/10.1016/j.jobe.2022.104264

Smart Evaluation of Building Fire Scenario and Hazard by Attenuation of Alarm Sound Field

Caiyi Xiong[1,2], Zilong Wang[1], Yunke Huang[3], Fan Shi[3], Xinyan Huang[1,*]

[1]*Department of Building Environment and Energy Engineering, Hong Kong Polytechnic University, Hong Kong*

[2]*The Hong Kong Polytechnic University Shenzhen Research Institute, Shenzhen, China*

[3]*Department of Mechanical and Aerospace Engineering, The Hong Kong University of Science and Technology, Hong Kong*

* Corresponding to xy.huang@polyu.edu.hk (X. Huang)

Abstract:

The audible fire alarm system of the building makes a sharp sound to alert all occupants when fires occur. According to the fire code, the fire alarm should be loud enough to be heard in any corner of the building. Thus, this work explores a smart technology of using alarm attenuation to reveal the fire scene information. Different alarms with frequencies from 500 to 2,000 Hz are tested. The propanol pool fires of different sizes and shapes are selected as the detecting targets. Results show that the sound pressure attenuation by the fire plume is positively correlated with the fire scene heat release rate. The sound-pressure attenuation is also greater if the flame thickness is larger along the sound path. Hence, a sound-field fire monitoring model is proposed and further verified by experiments using larger wood-crib fire and liquid-pool fire. This work provides a practical sound-based fire monitoring model and helps establish a scientific framework for the smart technology of using the existing audible alarm system to continuously monitor the building fire development.

Keywords: *building fire; fire detection; audible fire alarm; sound pressure; fire hazard*

Graphic Abstract

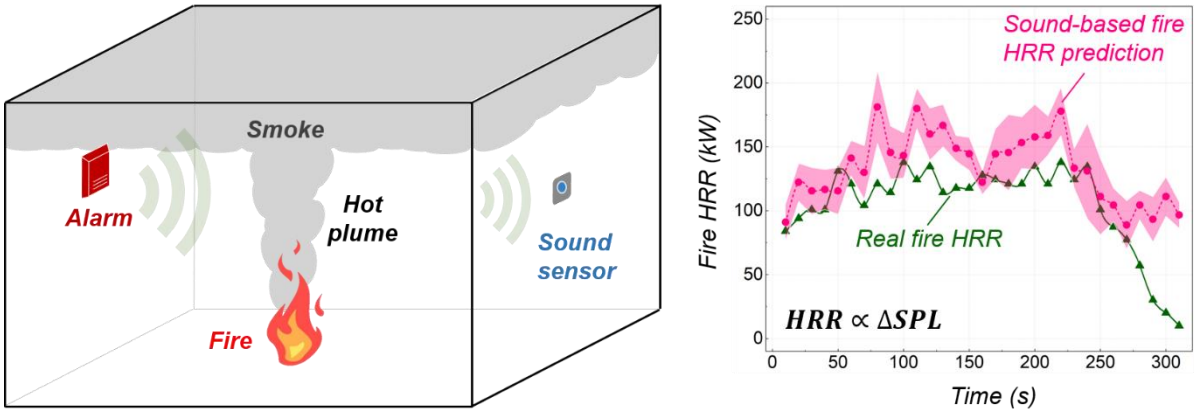

1. Introduction

A reliable method of identifying the complex fire scene and monitoring the fire development inside the building is commonly desired in fire protection and firefighting operations. As required by the fire codes, smoke, heat, and flame image detectors are installed in most modern buildings to detect the existence of fire (i.e., Yes or No) in the early fire stages [1–4]. However, these conventional fire detectors are not designed to provide additional information from the fire, such as the power and hazard of fire and the height of the smoke layer, and are easily damaged by high temperature and heat flux [5]. The CCTV camera network installed inside the building can help observe the fire scene, but the camera views are normally limited to public areas [6]. Also, cameras are often installed near the ceiling, so they are easily blocked by the heavy smoke from the fire. In sum, there are so far limited methods that can monitor the transient fire development and at the same time measure the real-time fire heat release rate (HRR) [2,7–9]. More methods are expected to improve the building fire response.

Fire is an extreme event that can significantly change the building environment, such as temperature, gas composition, luminance, and visibility [2–4]. As a result, quantifying the change of environment can help reveal critical fire information, which is the basis of different fire detection methods. As the sound, i.e., a longitudinal pressure wave [10,11], propagates in the air, the sound propagation velocity increases with the air temperature [12]. Since fire can significantly raise the temperature of the building environment, it is possible to detect fire by measuring the average sound velocity over the path across the fire scene. Such a technique, termed acoustic pyrometry [13–16], has been implemented and used to measure the flame and gas temperatures by measuring the average velocity of sound over the path through the flames in boiler and furnace [13]. However, this method requires a large fire size and multiple expensive sound-speed sensors to ensure accuracy. For a fire event that occurs at a random building room on any combustible, it is difficult to apply this velocity-based acoustic pyrometry.

Generally, the sound wave has two primary parameters, i.e., sound pressure and frequency [17]. Previously, the impact of fire on sound frequency has been extensively explored, motivated to improve the reliability of the personal alert safety system carried by firefighters for rapid positioning in the fire rescue [18,19]. It has been found that for an existing sound signal in a room, the rapid increase of room temperature at the moment of fire ignition will cause a frequency shift of the sound spectra towards a higher value, which was then used as the basis of an early-stage fire detection system [20]. However, this frequency-based system is only sensitive to the initial fire occurrence and cannot continue monitoring the building fire development.

In contrast, sound pressure is rarely used as a parameter for detection, let alone for building fire monitoring, even though it is the most easily measured parameter and requires no additional signal processing technology. Because fire plume is essentially a cloud of hot gas and is of a large density difference from cold air, it is expected that the fire plume can behave as a plate or wall to block part of sound, depending on the fire size and intensity, and thus causing an obvious sound pressure attenuation (i.e., variation in the sound pressure level, ΔSPL). Furthermore, if a correlation between the fire HRR

and the caused pressure attenuation can be established, this pressure-based technology can further reveal and continuously monitor the fire evolution [21]. Conveniently, the most common sound sources in modern buildings are the audible fire alarms, pre-installed on the sidewalls and ceilings [22–24]. In case of a fire, these alarms can emit a standard sound with sufficient energy to cover all building corners [25–28]. In this way, these fire alarms might have the potential to support acoustic-based fire monitoring, requiring only low-cost microphones (Mic) or other acoustic sensors from computers, mobile phones, and the Internet of Things (IoT) system already in the building [29].

Therefore, this paper explores a smart technology of using the pressure attenuation of fire alarm sound for monitoring the building fire HRR and evaluating fire hazards. The experiments first test the fires supported by propanol with different pool shapes and sizes. Alarm attenuations at different sound frequencies are measured to establish a model between the pressure attenuation ΔSPL and the fire HRR. A larger propanol-pool fire and wood-crib fire are also tested to validate if the proposed model can continuously predict the more complex fire HRR evolutions.

2. Experimental methods

2.1. Sound source and measurement

The experiment uses a sound source to emit acoustic waves to pass through the target fires, as illustrated in Fig. 1. To help build up the model, an adjustable source is first used, in which the acoustic signal is produced by a wave generator, enhanced by a power amplifier, and emitted as audible sound by a 2.5-inch (6.35-cm) diameter speaker. A commercial Honeywell alarm bell (SSV-series) with a pre-set working frequency and pressure is also used for model demonstration.

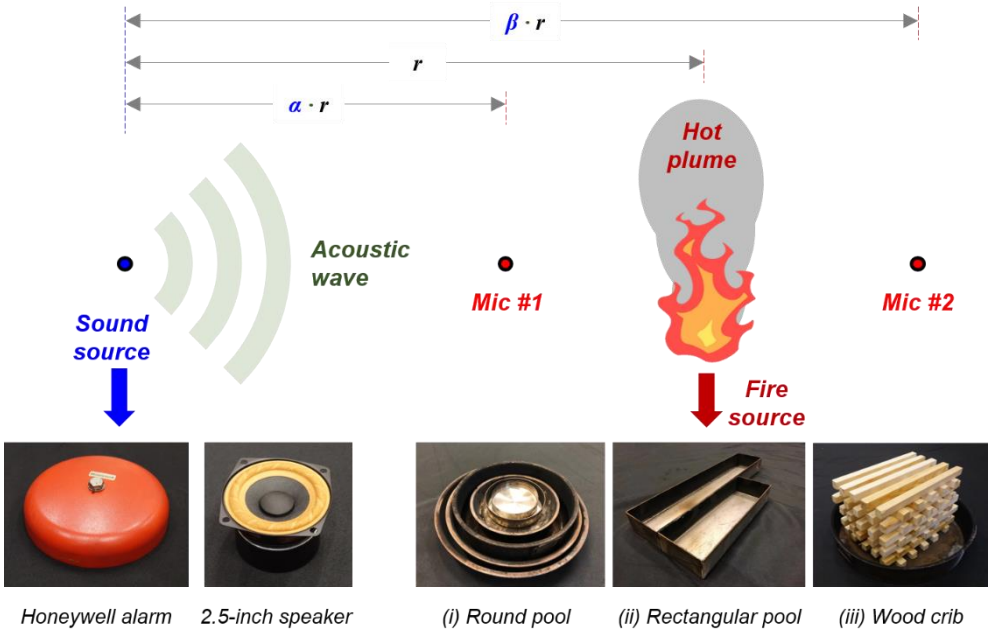

Fig. 1. The schematic of the experimental setup with different sound and fire sources.

To make the speaker-produced sound close to the real alarm but with flexible acoustic parameters, the requirements of both the alarm frequency and pressure in different building fire codes (HK [30],

UK [31], and US [32]) are referenced. In general, all codes recognize the alarm to have a duration of at least 60-s and usually last throughout the fire incident. For the alarm frequency, the UK code recommends a normal range from 500 – 1,000 Hz that is easily captured by human ears. The HK and US codes give no prescribed frequency but only suggest being higher than the background noise picket.

As for the alarm SPL, both the HK and UK codes recommend a range from 65 – 120 dB, while the US code requires 5 – 15 dB higher than the background noise. If considering the elder group or equipment aging, a higher alarm SPL range from 75 – 120 dB is recommended [26]. Combined, the speaker used produces a sound with an SPL of 93 dB at 1 m distance, which also covers an area within a radius of 8 m with an SPL larger than 75 dB. As for the sound frequency, an extensive range based on code recommendation, 500 – 2,000 Hz, was used, which helps check the impact of alarm frequency on the proposed technique. Measurement of the sound signal is completed by the KM-2 free-field Mic placed in the test room. Digitization of the signal received is carried out by an audio card. The pressure attenuation of the signal is measured by a post-processing program installed on the computer, which calculates the signal transfer function in real-time.

2.2. Tested fire sources

The tested fires include the one produced by propanol pool at different shapes and sizes, and the other supported by a scaled wood crib (30cm×20cm×20cm) used in the British fire standard (BS8414-2) [33], seen in Fig. 1. The small round pools, with diameters from 9 – 28 cm, are first used to study the influence of fire HRR on the alarm ΔSPL. Then, two rectangular pools, with the same width of 10 cm but different lengths of 30 and 50 cm, are used to investigate the influence of fire geometry (width, length, and height) on the alarm ΔSPL. Afterwards, the larger fires supported by a 41-cm round pool and wood crib are used for model demonstration.

Table 1. Parameters for the tested fuels, fires, and sound sources.

Exp. group	Fuel	Pool shape	Fuel size * [cm]	Fuel mass loss rate [g/s]	Fire HRR [kW]	Sound source	Research purpose
a	Propanol	Round	9	0.07	2.5	2.5-inch speaker	Check the impact of fire HRR on ΔSPL
			12	0.14	4.6		
			14	0.19	6.4		
			18	0.55	19.5		
			22	0.80	26.9		
			28	0.96	32.4		
b	Propanol	Rectangular	30 × 10	0.34	11.4	2.5-inch speaker	Check the impact of fire geometry on ΔSPL
			50 × 10	0.62	20.9		
c	Propanol	Round	41	3.53	121.6	Alarm bell	Model verification
	Wood	Cubic	50×10×20	6.01	105.8		

* Round pool diameter; length × width of rectangular pool; heat of combustion: 33.6 kJ/g (propanol) and 18.0 kJ/g (wood) [34].

To confirm the repeatability of the experiment, the fuel in all pools keeps 1-cm deep, which allows for a stable burning for more than 1 min in different trials (see the measured fuel mass-loss rates in Fig. A1). The fire HRR increases with the pool size, ranging from 2.5 kW (9-cm pool) to 121.6 kW (41-cm pool). Because the stable burning always occurs at about 60 s after ignition, the alarm ΔSPL during the stable burning stage is measured. All fuel- and fire-related parameters are given in Table 1.

2.3. Experimental procedure

All experiments are conducted in a large fire test room with a size of 8 m (length) × 5 m (width) × 3 m (height). Three groups of tests are conducted: (a) round pool fire with an adjustable speaker, (b) rectangular pool fire with an adjustable speaker, and (c) large fires with a standard alarm bell (Fig. 2).

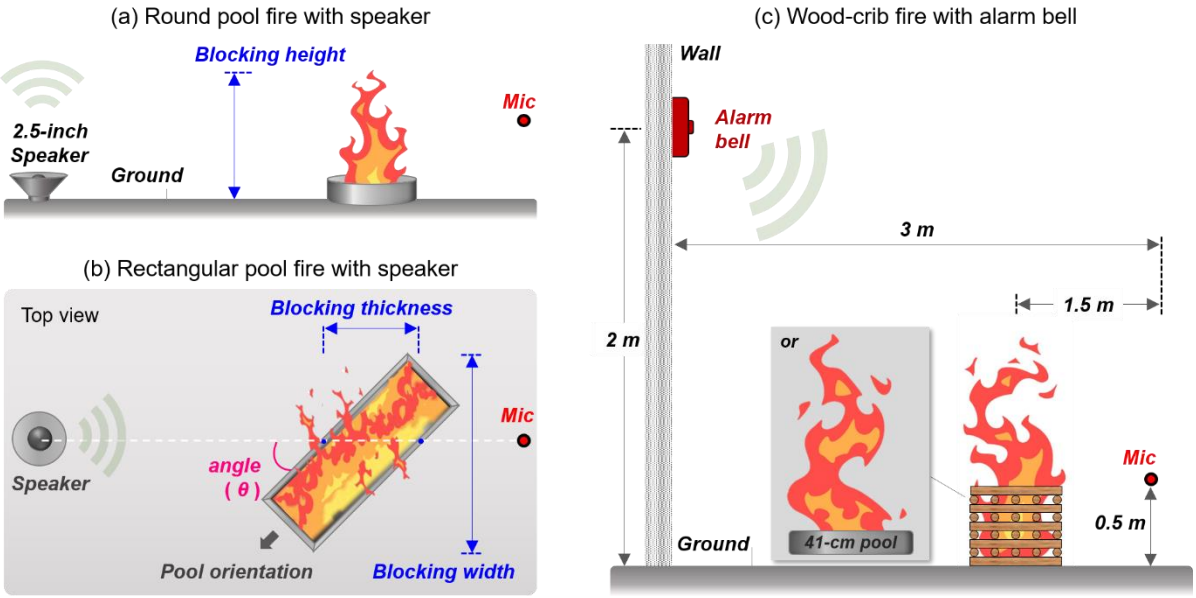

Fig. 2. Setups of test groups (a) round pool fire with a speaker, (b) rectangular pool fire with a speaker, and (c) large fires with a standard fire alarm bell for model verification.

In Group (a), the fire HRR varies with the pool diameter. The fire is set on the floor in the center of the room. To help build up the monitoring model, the adjustable speaker is placed on the floor with its diaphragm facing upward. Such a configuration can produce simplified hemispherical sound waves and moderate the impact of sound directivity [18]. Here, two Mics in line with the speaker are first used to help quantify the distribution of alarm sound in the tested room (Fig. 1). Then, only one Mic after the fire is left and used to evaluate the fire-induced alarm ΔSPL (Fig. 2a). The height of Mic is at least 30 cm above the floor to avoid sound blocked by the pool edge.

In Group (b), rotating the rectangular pool can easily change the fire geometry without changing fire HRR. When changing the pool orientation angle (θ), two fire geometry parameters (fire blocking width and thickness) also change, which can be calculated. Usually, the larger the fire HRR, the higher the fire height. Thus, the information of fire height can be covered by the fire HRR variation.

In Group (c), a Honeywell alarm bell installed on the sidewall with a height of 2-m to the floor is

used, mounted 3-m away from bell and 0.5-m to the floor. The target fire is between the bell and Mic.

Before tests, the background noise in the test room is measured to be around 45 dB and lower than 30 Hz. The noise generated by buoyant fire puffing is also quantified, which is very close to that of the room background noise, as shown in Appendix (Fig. A2). Thus, the influence of background noise is negligible, which does not significantly affect alarm-based monitoring. During experiments, the speaker is activated first to produce sound with pre-defined frequency and SPL. After the fire develops to a stable stage, the Mic starts to receive the local sound signal and transfer data to the post-processing system to calculate ΔSPL. The whole monitoring process lasts for 60 s, and each trial is repeated three times to reduce the uncertainty by fire puffing.

3. Experimental results

3.1. Natural sound attenuation vs. fire-induced attenuation

As seen in Fig. 1, the spacing between the fuel pool and speaker is defined as r, and the spacings between the speaker and two Mics are given as $\alpha \cdot r$ and $\beta \cdot r$. The initial experiment using a 1,000-Hz sound and an 18-cm round pool is selected as the base case to begin with. This base case is first carried out to check whether a fire can block the alarm and cause an obvious ΔSPL as expected. Here, the speaker-fire spacing is fixed at r = 1.5 m, and two Mics are mounted at 1 m and 2 m away from the speaker, leading to α = 0.66 and β = 1.32, based on the spacing ratio given in Fig. 1.

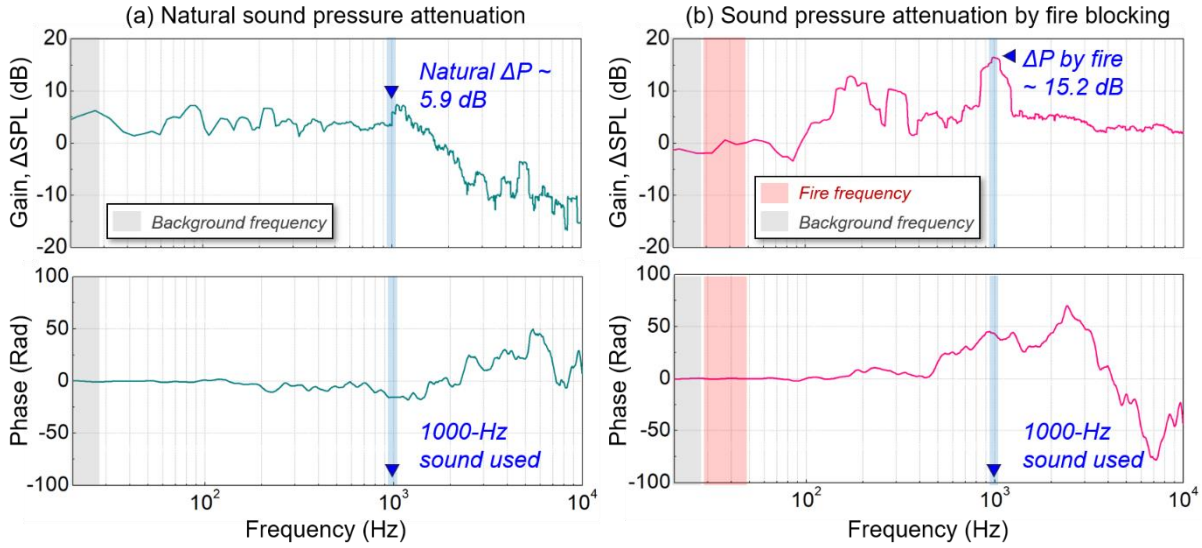

Fig. 3. A comparison of the gain and phase between the sound received by two different Mics in test room (a) without and (b) with an 18-cm pool fire.

To characterize the sound field in the test room, the 2.5-inch speaker is activated to produce a 1,000-Hz sound with specific SPL, and the natural pressure attenuation (ΔSPL) in the test room is quantified by the two Mics. Fig. 3a shows both ΔSPL and phase changes between the signals received by Mics #1 and #2, where ΔSPL can keep around 6 dB in a wide frequency band. This confirms that

the small speaker can behave as a point source to produce hemisphere waves, where the SPL decreases by 6 dB every time the distance from the source is doubled [32]. Also, the phase variation near the target frequency is almost zero, demonstrating that the sound reflection in the test room has only little effect on the experiment.

Then the 18-cm pool is ignited to produce fire to block the 1,000-Hz sound. The ΔSPL and phase changes between two Mics are given in Fig. 3b. It is seen that, compared with the natural attenuation ΔSPL, the fire-induced attenuation ΔSPL is increased almost in the whole frequency band. Particularly, the maximum attenuation ΔSPL occurs at the target frequency 1,000 Hz, increased from 5.9 dB to 15.2 dB, which equals a pressure difference of 0.29 Pa. This observation confirms the ability of the fire and its hot plume to attenuate alarm pressure. The mechanism behind this fire-induced attenuation can probably be attributed to acoustic scattering because the pool-fire sheet is not perfectly homogeneous. However, details of this mechanism require future study, but it has no impact on the current applied research. As a result, the technique of using alarm pressure attenuation to monitor a fire is feasible.

3.2. Alarm pressure attenuation vs. fire HRR

As the fire HRR is the key information of a fire scene, the correlation between alarm ΔSPL and fire HRR is explored. The Group (a) experiments, which are expanded from the base case, are then carried out. More round pools with diameters from 9 – 28 cm are used here (Fig. 4a). Specifically, only one Mic after fire is left to measure alarm ΔSPL. Fig. 4b shows all the measurements plotted versus the fire HRR measured in the stable burning stage.

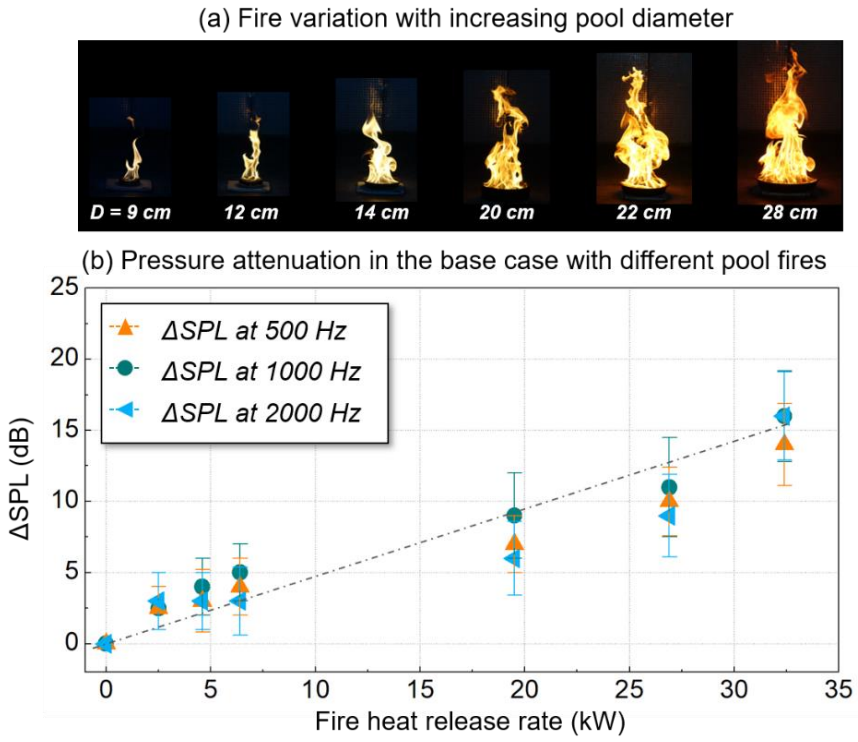

Fig. 4. (a) Target pool fires, and (b) dependence of ΔSPL on fire HRR at different frequencies by one Mic.

As expected, the fire with a larger HRR can cause a greater ΔSPL, which forms a basis on which to carry out the pressure-based fire monitoring technology. Note that the measuring error increases as the fire HRR increases. This is because the larger the fire, the louder noise the fire will generate to interfere with the sound field. To further quantify the influence of sound frequency, two different frequencies at 500 and 2,000 Hz are tested. Fig. 4b compares the trends at different frequencies, where the positive correlation between ΔSPL and fire HRR does not change.

3.3. Sound pressure attenuation vs. fire geometry

So far, all the measuring data are only applicable to ideal fire cases, i.e., round pool fires. In practice, room fire is usually supported by irregular fuels. Re-examining the fire shapes in Fig. 4a, when the pool diameter increases, the fire HRR increases, but the fire geometry also changes, represented by three geometry parameters: fire blocking width, thickness, and height (see Fig. 2). In this way, in addition to the fire HRR, Group (b) experiments with rectangular pool fires are used to study the influence of fire geometry on ΔSPL.

Fig. 5a shows the measured ΔSPL by the same Mic after fire when changing the pool angle under a 1,000-Hz sound. The most prominent feature in Fig. 5a is that, although the fire HRR of the rectangular pool is fixed, the fire-induced ΔSPL still shows a dependence on the fire geometry. In particular, the fire blocking thickness has a greater impact on ΔSPL than the other two geometry parameters, as evidenced by the difference in ΔSPL in Fig. 5a when using different rectangular pools, i.e., the ΔSPL measurements have a difference of 7 dB at $\theta = 0^{\circ}$, caused by the increase in fire blocking thickness from 30 cm to 50 cm, which is much larger than the differences at other pool angles θ, see Fig. 5b. Thus, the fire HRR and fire blocking thickness are the two main factors to affect the alarm attenuation ΔSPL.

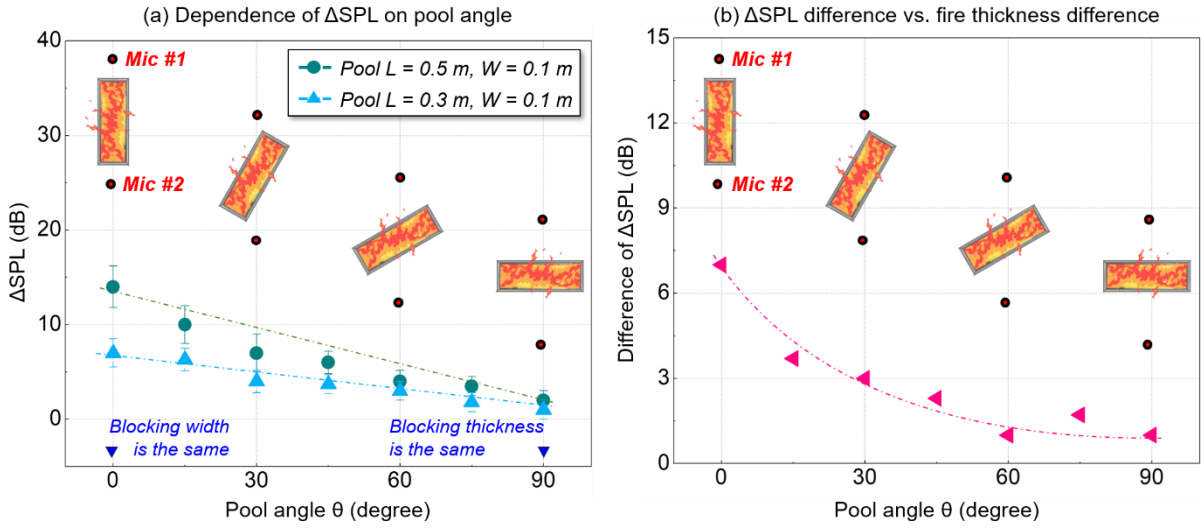

Fig. 5. Dependences of (a) alarm attenuation and (b) difference in the alarm attenuation on pool angle.

4. The pressure-based fire monitoring model

4.1. Model formulation

Re-examining Fig. 1. Based on the acoustic fundamentals [35], the initial sound intensities at Mic #1 and #2 without fire are

$$I_{mic1} = \frac{S}{2\pi(\alpha r)^2} \tag{1}$$

$$I_{mic2} = \frac{S}{2\pi(\beta r)^2} \tag{2}$$

where S denotes the sound source power, and the denominators denote the area of the hemispherical sound waves. Then, the natural attenuation ΔSPL between Mics #1 and #2 can be

$$\Delta SPL_N = 10 \cdot log_{10}\left(\frac{I_{mic1}}{I_{mic2}}\right) = 20 \cdot log_{10}\left(\frac{\beta}{\alpha}\right) \tag{3}$$

As seen, Eq. (3) is irrelative to the source power, which depends only on the Mic spacing. In the initial base experiment, the Mic spacing is in a double-distance condition [32], i.e., $\beta = 2\alpha$, so ΔSPL_N keeps around 6 dB.

The appearance of fire can change Eq. (2). Since fire is essentially a high temperature gas, it has a density vastly different from surrounding cold air. To expose the idea, the concept of light transmission is borrowed. The small speaker, which is a point sound source, can be viewed as a point source of light here, and the fire and its hot plume can be considered as a light-transmitting glass wall. In this way, a transmission coefficient Γ can be added to Eq. (2), which represents the relative intensity of the sound wave that passes through the fire and reach Mic #2:

$$I_{mic2,f} = \frac{\Gamma \cdot S}{2\pi(\beta r)^2} \tag{4}$$

As a result, the measured ΔSPL becomes

$$\Delta SPL = 10 \times log_{10}\left(\frac{I_{mic1}}{I_{mic2,f}}\right) = 20 \cdot log_{10}\left(\frac{\beta}{\alpha}\right) + 10 \cdot log_{10}\left(\frac{1}{\Gamma}\right) \tag{5a}$$

Based on Eq. (5a), the measured ΔSPL in experiments between Mic #1 and #2 in Fig. 1 is found to consist of two parts: 1) the natural pressure attenuation caused by Mic spacing (ΔSPL_N in Eq. 3), and 2) the attenuation caused by fire blocking (or transmission), given as $10 \cdot log_{10}(1/\Gamma)$.

On the other hand, Eq. (5a) can be written as

$$\Delta SPL = 10 \times log_{10}\left(\frac{I_{mic1}}{I_{mic2}} \times \frac{I_{mic2}}{I_{mic2,f}}\right) = 10 \cdot log_{10}\left(\frac{I_{mic1}}{I_{mic2}}\right) + 10 \cdot log_{10}\left(\frac{I_{mic2}}{I_{mic2,f}}\right) \tag{5b}$$

A comparison between the right-hand side of Eqs. 5a-b allows finding that the alarm attenuation by fire blocking, i.e., $10 \cdot log_{10}(1/\Gamma)$, can be measured using only one Mic behind the fire (i.e., Mic #2), as

$10 \cdot log_{10}(I_{mic2}/I_{mic2,f})$. In this way, if only using Mic #2 to monitor fire, the measured ΔSPL is

$$\Delta SPL = 10 \times log_{10}\left(\frac{I_{mic2}}{I_{mic2,f}}\right) = 10 \cdot log_{10}\left(\frac{1}{\Gamma}\right) \quad (6)$$

In either case, the coefficient Γ is a parameter that has to be modelled. Based on the previous discussion, it is known that there are two fire-related factors to affect ΔSPL, i.e., fire HRR and blocking thickness ΔL. Thus, Γ can be expressed as a function as

$$\Gamma = \Gamma(HRR, \Delta L) \quad (7)$$

Note that although HRR and ΔL may be coupled with each other, writing them separately can provide convenience to build the model. Besides Eq. (7), Γ must meet two boundary conditions:

$$\Gamma(HRR, \Delta L)|_{HRR=0} = 1 \quad (8a)$$

$$\Gamma(HRR, \Delta L)|_{\Delta L=0} = 1 \quad (8b)$$

which means that if there is no fire, the pressure attenuation by fire blocking should be zero. Since Γ should be negatively correlated with HRR and ΔL, and combined with the boundaries Eqs. 8a-b, it can be confirmed that Eq. (7) is an exponential function and both HRR and ΔL are the exponents.

Since Γ is initially introduced by borrowing the concept of light transmission into the current work, the Beer-Lambert law [36,37], which describes the light transmission based on the properties of the material through which the light is travelling, is also borrowed to help obtain Eq. (7)

$$T = 10^{-\varepsilon \cdot c \cdot z} \quad (9)$$

where T is the transmittance of the material; ε, c, z are the molar attenuation coefficient, concentration, and traveling path length of light in the material. As can be seen, both Γ in Eq. (7) and T in Eq. (9) have essentially the same mathematical features, and they are all used to describe the wave attenuation in the material. Thus, Eq. (7) is expanded in the same exponential form as

$$\Gamma = 10^{-a \cdot HRR \cdot \Delta L} \quad (10)$$

where a is a fitted coefficient analogous to the molar attenuation coefficient ε, HRR mimics the material (plume or smoke) concentration c, and ΔL mimics the path length z in the Beer-Lambert law [36,37]. By combining Eqs. 6 and 9, the pressure-based fire monitoring model using one Mic becomes

$$\Delta SPL = 10 \cdot a \cdot HRR \cdot \Delta L \quad (11)$$

Fig. 6a shows the calculation of the coefficient a in Eq. (11) based on the data from Fig. 4b. It is seen that a is not constant but is negatively correlated with fire HRR. However, what a mimics is the molar attenuation coefficient ε in the Beer-Lambert law, which should have been constant. This is because as the fuel pool becomes larger, the fire will stay in different burning conditions. Although the fire is always fueled by propanol vapor, the increase in pool size will change it from a fuel-lean fire to a fuel-rich fire, evidenced by the color change of fire in Fig. 4a.

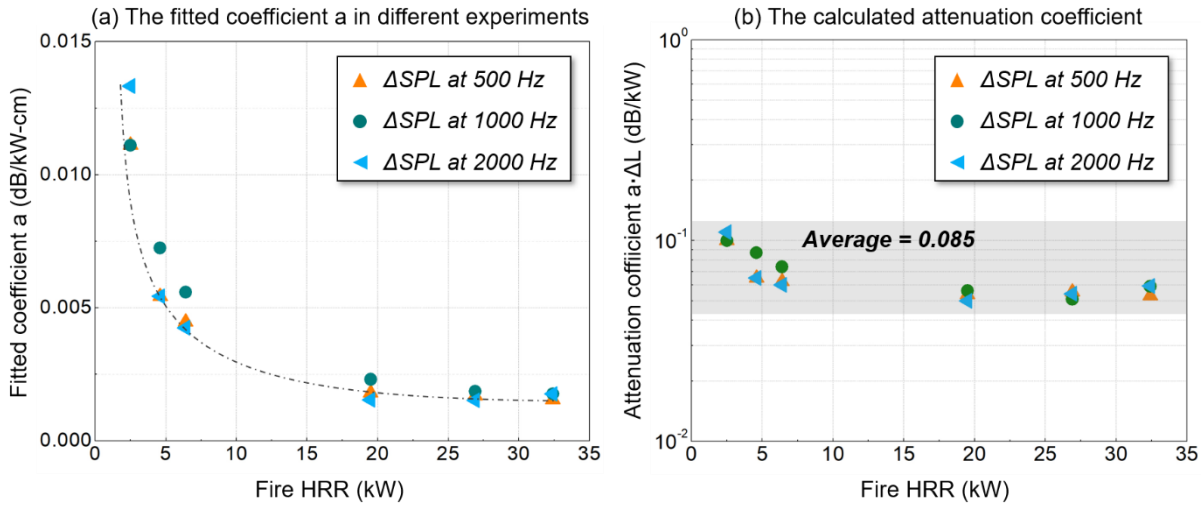

Fig. 6. (a) The fitted coefficient a and (b) attenuation coefficient $a \cdot \Delta L$ by various experiments.

Although there is no constant a to fit Eq. (11), it is found that the product of coefficient a and fire blocking thickness ΔL, i.e. $a \cdot \Delta L$, can be a value concentrated around 0.085, see Fig. 6b. In fact, this combined term is formulated based on the Napierian attenuation coefficient in Lambert's law [36,37]. It can be seen that the unit of $a \cdot \Delta L$ is dB/kW, which reflects the attenuation of alarm pressure per each 1 kW of fire. Eventually, the demand fire monitoring model using only one Mic behind fire is established as

$$HRR = \frac{\Delta SPL}{0.085} \tag{12}$$

which can give a stable prediction with the measurement uncertainty of about 10%.

4.2. Model verification and perspectives

To verify Eq. 12, Group (c) experiments are carried out with larger fires to mimic real building fire scenarios, see Fig. 7a, in which a 41-cm pool fire and a wood crib fire are separately used as the target. The alarm source changes to use a standard alarm bell installed on the sidewall, with the peak frequency measured to be around 2,120 Hz.

Figs. 7b-c compare the instant ΔSPL measured by the Mic at 3-m from the bell. Overall, with the sound emitting from the alarm bell, the fire can cause an overall increase in the ΔSPL in a wide frequency range, which again confirms the feasibility of such a pressure-based method. Specifically, the fire-induced attenuation ΔSPL at 2,120 Hz is the largest, recorded every 10 s with the uncertainty calculated from the local 1-s signal piece. These data are then used to fit Eq. (12) to predict the overall fire HRR evolution from initial fire ignition to final extinction. To further validate the monitoring model (Eq. 12), data from another Mic mounted at 4-m from the bell are also used. Fig. 8 shows a comparison of the measured fire HRR evolution (coming from the product of fuel mass loss rate and heat of combustion, Fig. A1) and the predicted ones by Eq. (12). It is found that the proposed model (Eq. 12) can effectively evaluate the hazard level as the fire develops.

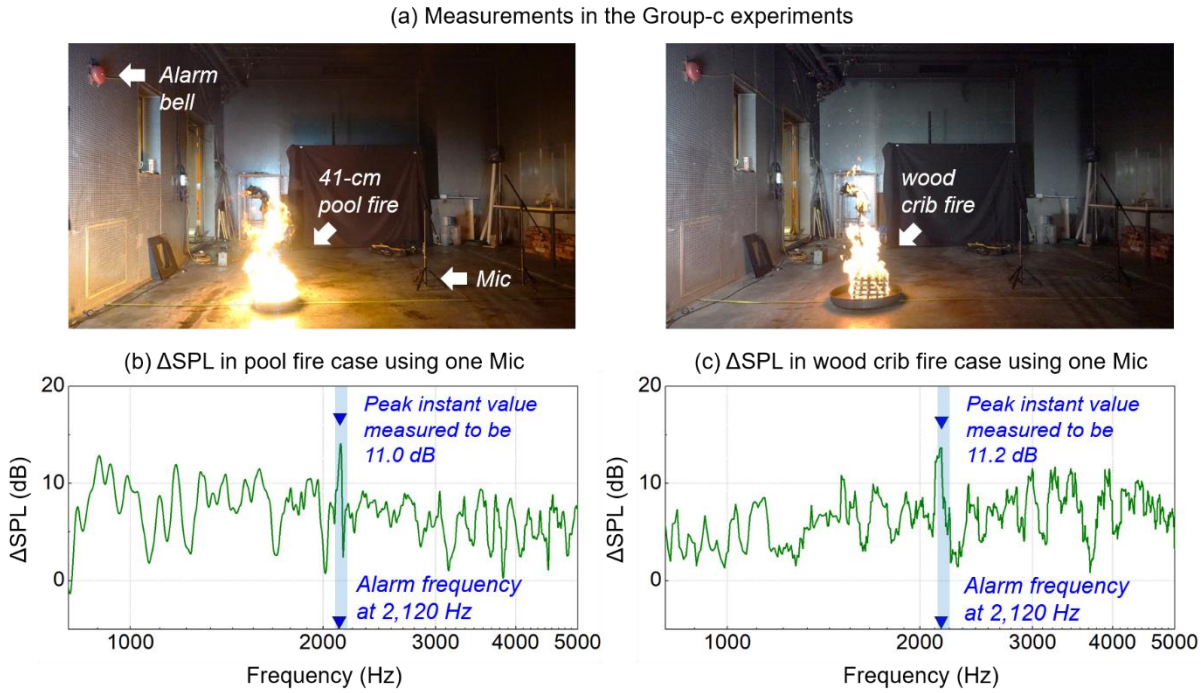

Fig. 7. (a) Measurements in the Group-c experiments, and the instant ΔSPL received by the Mic after (b) 41-cm pool fire and (c) wood-crib fire.

Note that the existing fire detection devices, such as smoke, heat and flame detectors, and CCTV cameras, can only tell the existence of fire (e.g., Yes or No) but can neither tell how big the fire is nor how fast the fire is growing. Comparatively, the proposed smoke fire monitoring system, based on the change of alarming sound field, can provide more information about fire scenarios for firefighting and rescue operations. Moreover, other optical-based detectors and CCTV cameras will soon be covered by smoke layer [38] and lose the monitoring capability in the early stage of fire. Nevertheless, the proposed smart acoustic system can continuously monitor the development of and evaluate the fire scene covered by an invisible smoke layer until all sensors are physically destroyed by fire.

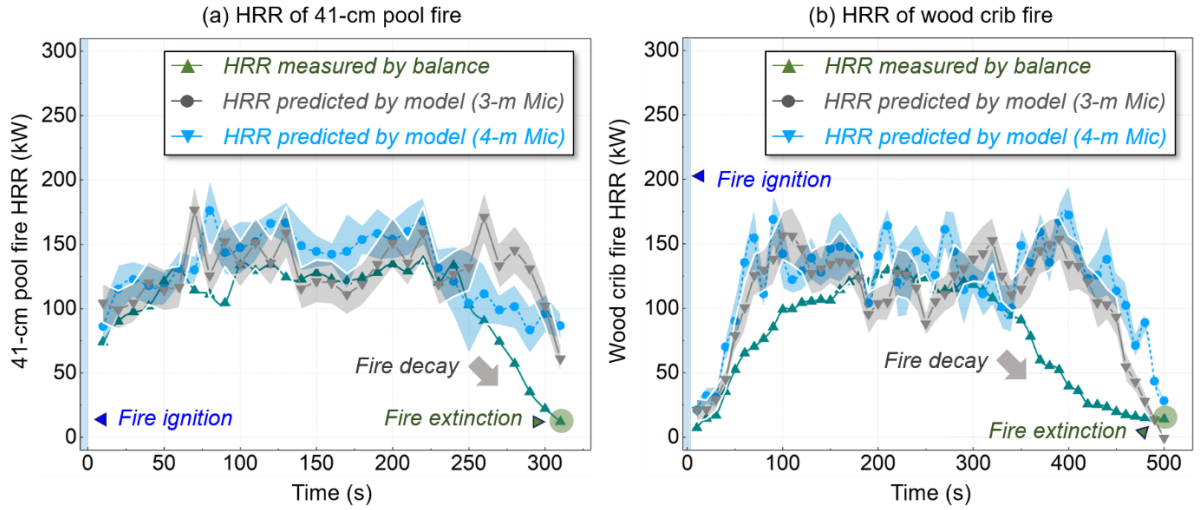

Fig. 8. Evolution of fire HRR from ignition to extinction by model prediction and balance measurement for (a) 41-cm pool fire and (b) wood crib fire.

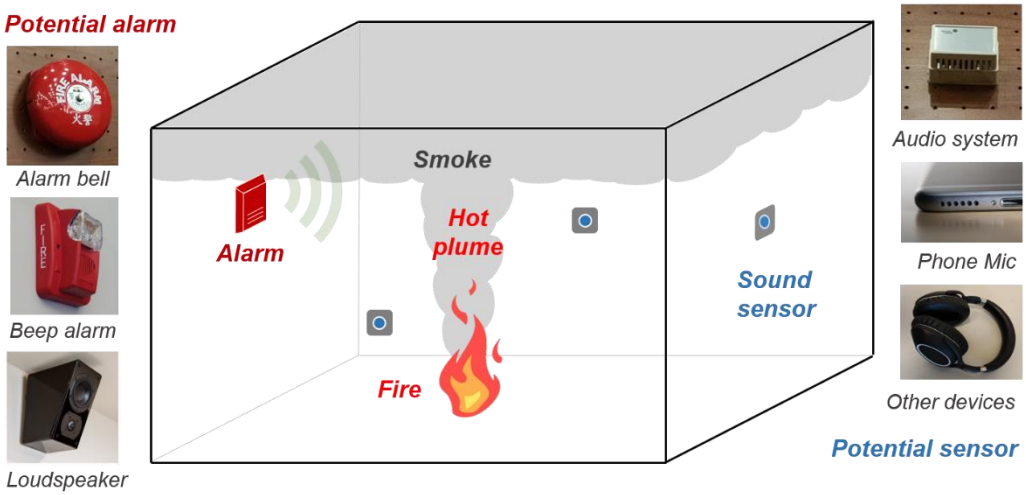

Fig. 9. The potential application of the alarm-based fire monitoring technology based on the existing sensors and alarm in the building.

Today, more and more sensors are adopted in buildings to achieve intelligence, resilience, and sustainability. Different kinds of microphones are available inside the building, such as the mics in everyone's smartphone and laptop, as well as the audio system (e.g., in the classroom), as illustrated in Fig. 9. Most of these mics are low cost and can be connected to the existing fire detection system or the future smart IoT system. Thus, the proposed smart fire monitoring technique by measuring the sound field has unique advantages and a great potential for applying in future smart firefighting systems.

5. Conclusions

This paper carried out an experimental investigation of using audible fire alarm sound to monitor the existence of building fire and continuously evaluate the fire-scene hazard. The pressure attenuation of the alarm sound by fire blocking is used as the primary monitoring parameter. The tested alarm sources include a 2.5-inch flexible speaker and a commercial Honeywell alarm bell (500-2,000 Hz), and fire sources include different propanol pool fires and wood-crib fires up to 200 kW.

The correlation between alarm ΔSPL and fire is first explored. Experiments using round pool fires indicate that the fire with a larger HRR can cause a greater alarm ΔSPL. Experiments using rectangular pool fires further indicate that the alarm ΔSPL is positively correlated with the fire blocking thickness ($\Delta SPL \propto HRR$). On the ground of this, a simplified but practical alarm pressure-based building fire monitoring model is proposed, further verified by experiments using large propanol-pool fire and wood-crib fire. Results prove that the proposed model can continuously evaluate the fire HRR from ignition to extinction in real building fire scenarios without interference by the fire smoke. The proposed fire-monitoring technology could be part of the future smart firefighting system driven by IoT sensor networks and AI algorithm.

This work provides a promising smart technology for monitoring building fire based on the existing fire alarm system, which helps expand the conventional channel to non-intrusively evaluate building

fire development. Considering the sound field is sensitive to the variation in the environment temperature, further research on using the alarm sound to evaluate the fire smoke properties like smoke thickness or height seems reasonable.

Acknowledgments

CX is funded by the National Natural Science Foundation of China (NSFC) Grant No. 52006185. XH is funded by the Hong Kong Research Grants Council Theme-based Research Scheme (T22-505/19-N) and HK PolyU Emerging Frontier Area (EFA) Scheme of RISUD (P0013879).

CRediT authorship contribution statement

Caiyi Xiong: Investigation, Writing-original draft, Formal analysis, Funding acquisition.

Zilong Wang: Investigation, Formal analysis, Resources.

Yunke Huang: Investigation, Formal analysis, Resources.

Fan Shi: Methodology, Formal analysis, Writing-review & editing.

Xinyan Huang: Conceptualization, Supervision, Formal analysis, Writing-review & editing, Funding acquisition.

Conflicts of interest

The authors declare that they do not have any conflicts of interest.

References

[1] A. Gaur, A. Singh, A. Kumar, A. Kumar, K. Kapoor, Video Flame and Smoke Based Fire Detection Algorithms: A Literature Review, Fire Technol. 56 (2020) 1943–1980. doi:10.1007/s10694-020-00986-y.

[2] Z. Wang, T. Zhang, X. Wu, X. Huang, Predicting transient building fire based on external smoke images and deep learning, J. Build. Eng. 47 (2022) 103823. doi:10.1016/j.jobe.2021.103823.

[3] M.A.M.S. Shoshe, M.A. Rahman, Improvement of heat and smoke confinement using air curtains in informal shopping malls, J. Build. Eng. (2021) 103676. doi:10.1016/j.jobe.2021.103676.

[4] R. Ouache, K.M. Nahiduzzaman, K. Hewage, R. Sadiq, Performance investigation of fire protection and intervention strategies: Artificial neural network-based assessment framework, J. Build. Eng. 42 (2021) 102439. doi:10.1016/j.jobe.2021.102439.

[5] F.F. Chen, Y.J. Zhu, F. Chen, L.Y. Dong, R.L. Yang, Z.C. Xiong, Fire Alarm Wallpaper Based on Fire-Resistant Hydroxyapatite Nanowire Inorganic Paper and Graphene Oxide Thermosensitive Sensor, ACS Nano. 12 (2018) 3159–3171. doi:10.1021/acsnano.8b00047.

[6] A.E. Çetin, K. Dimitropoulos, B. Gouverneur, N. Grammalidis, O. Günay, Y.H. Habiboğlu, B.U. Töreyin, S. Verstockt, Video fire detection - Review, Digit. Signal Process. A Rev. J. 23 (2013) 1827–1843. doi:10.1016/j.dsp.2013.07.003.

[7] X. Wu, X. Zhang, Y. Jiang, X. Huang, G.G.Q. Huang, A. Usmani, An intelligent tunnel firefighting system and small-scale demonstration, Tunn. Undergr. Sp. Technol. 120 (2022)

104301. doi:10.1016/j.tust.2021.104301.

[8] W.C. Tam, E.Y. Fu, R. Peacock, P. Reneke, J. Wang, J. Li, T. Cleary, Generating Synthetic Sensor Data to Facilitate Machine Learning Paradigm for Prediction of Building Fire Hazard, Fire Technol. (2020). doi:10.1007/s10694-020-01022-9.

[9] J. Baek, T.J. Alhindi, Y.S. Jeong, M.K. Jeong, S. Seo, J. Kang, W. Shim, Y. Heo, Real-time fire detection system based on dynamic time warping of multichannel sensor networks, Fire Saf. J. 123 (2021) 103364. doi:10.1016/j.firesaf.2021.103364.

[10] A. Glowacz, R. Tadeusiewicz, S. Legutko, W. Caesarendra, M. Irfan, H. Liu, F. Brumercik, M. Gutten, M. Sulowicz, J.A. Antonino Daviu, T. Sarkodie-Gyan, P. Fracz, A. Kumar, J. Xiang, Fault diagnosis of angle grinders and electric impact drills using acoustic signals, Appl. Acoust. 179 (2021) 108070. doi:10.1016/j.apacoust.2021.108070.

[11] A. Glowacz, Diagnostics of Direct Current machine based on analysis of acoustic signals with the use of symlet wavelet transform and modified classifier based on words, Eksploat. i Niezawodn. 16 (2014) 554–558.

[12] S.W. Rienstra, A. Hirschberg, An Introduction to Acoustics, Eindhoven University of Technology, 2020.

[13] T.A. Hanson, N. Yilmaz, P. Drozda, W. Gill, T.J. Miller, A.B. Donaldson, Acoustic pyrometry using an off-the-shelf range finding system, J. Fire Sci. 26 (2008) 287–308. doi:10.1177/0734904107087817.

[14] Q. Kong, G. Jiang, Y. Liu, M. Yu, Numerical and experimental study on temperature field reconstruction based on acoustic tomography, Appl. Therm. Eng. 170 (2020) 114720. doi:10.1016/j.applthermaleng.2019.114720.

[15] C. Kwan, X. Zhang, R. Xu, Early fire detection using acoustic emissions, IFAC Proc. Vol. 36 (2003) 351–355. doi:10.1016/S1474-6670(17)36516-3.

[16] Y.G. Sahin, T. Ince, Early forest fire detection using radio-acoustic sounding system, Sensors. 9 (2009) 1485–1498. doi:10.3390/s90301485.

[17] T. Yamazaki, T. Matsuoka, Y. Nakamura, Dynamic response of non-premixed flames subjected to acoustic wave, 12th Asia-Pacific Conf. Combust. ASPACC 2019. (2019).

[18] A.M. Z, S.J. I, W.P. S, Compartment fire growth effects on firefighter alarm signal detection, Proc. ASME 2013 Int. Mech. Eng. Congr. Expo. (2013) 1–10. doi:10.1115/IMECE2013-66367.

[19] M.Z. Abbasi, P.S. Wilson, O.A. Ezekoye, Change in acoustic impulse response of a room due to a fire, J. Acoust. Soc. Am. 147 (2020) 0–2. doi:10.1121/10.0001415.

[20] K.H. Park, S.Q. Lee, Early stage fire sensing based on audible sound pressure spectra with multi-tone frequencies, Sensors Actuators, A Phys. 247 (2016) 418–429. doi:10.1016/j.sna.2016.06.002.

[21] C. Xiong, H. Fan, X. Huang, C. Fernandez-Pello, Evaluation of burning rate in microgravity based on the fuel regression, flame area, and spread rate, Combust. Flame. 237 (2022) 111846. doi:10.1016/j.combustflame.2021.111846.

[22] J.H. Jeong, Prediction and Reduction of Alarm Sound Propagation Through Escape Stairways, Fire Technol. (2021). doi:10.1007/s10694-021-01131-z.

[23] M. Lee, Subjective Response to the Conditions of Audible Fire Alarm Signals Through a Jury Evaluation Test, Fire Technol. (2021). doi:10.1007/s10694-021-01186-y.

[24] I. Thomas, D. Bruck, Awakening of sleeping people: A decade of research, Fire Technol. 46 (2010) 743–761. doi:10.1007/s10694-008-0065-5.

[25] D.A. Robinson, Sound attenuation in buildings: Implications for fire alarm system design, Fire Saf. J. 14 (1988) 5–12. doi:10.1016/0379-7112(88)90040-9.

[26] L.T. Wong, L.K. Leung, Minimum fire alarm sound pressure level for elder care centres, Build. Environ. 40 (2005) 125–133. doi:10.1016/j.buildenv.2004.05.004.

[27] K.A.M. Moinuddin, D. Bruck, L. Shi, An experimental study on timely activation of smoke alarms and their effective notification in typical residential buildings, Fire Saf. J. 93 (2017) 1–11. doi:10.1016/j.firesaf.2017.07.003.

[28] A.M. Hasofer, I.R. Thomas, Sound intensity required for waking up, Fire Saf. J. 42 (2007) 265–270. doi:10.1016/j.firesaf.2006.11.005.

[29] J. Hu, J. Wu, X. Shu, S. Shen, X. Ni, J. Yan, S. He, Analysis and prediction of fire water pressure in buildings based on IoT data, J. Build. Eng. 43 (2021) 103197. doi:10.1016/j.jobe.2021.103197.

[30] Hong Kong Fire Services Department, Codes of practice for minimum fire service installation, (1998).

[31] British Standard Institution, BSI Standards Publication Fire detection and fire alarm systems for buildings – Part 1, BSI Stabdards Publ. (2013).

[32] National Fire Alarm and Signaling Code, NAPA 72: National Fire Alarm and Signaling Code, 2010.

[33] British Standard Institution, BS 8414-2 Fire performance of external cladding systems, (2015).

[34] Y. Ohmiya, S. Kang, M. Noaki, M.A. Delichatsios, Effects of opening aspect ratio on facade gas temperatures with and without sidewalls for underventilated conditions, Fire Saf. J. 113 (2020) 102944. doi:10.1016/j.firesaf.2019.102944.

[35] S.W. Rienstra, A. Hirschberg, An Introduction to Acoustics, Instituut Wiskundige Dienstverlening, 1992. doi:10.1063/1.3067395.

[36] D.F. Swinehart, The Beer-Lambert law, J. Chem. Educ. 39 (1962) 333–335. doi:10.1021/ed039p333.

[37] K. Locharoenrat, Optical Properties of Solids, 2016. doi:10.1201/b21205.

[38] J.G. Quintiere, Principles of Fire Behavior, 3rd ed., CRC Press, 2016.

[39] National Center for Environmental Health, What Noises Cause Hearing Loss?, U.S. Dep. Heal. Hum. Serv. (2019).

Appendix

Fig. A1a shows the measured mass loss rate when burning liquid propanol in different pools and burning the wood crib. Fig. A1b shows the corresponding fire heat release rate.

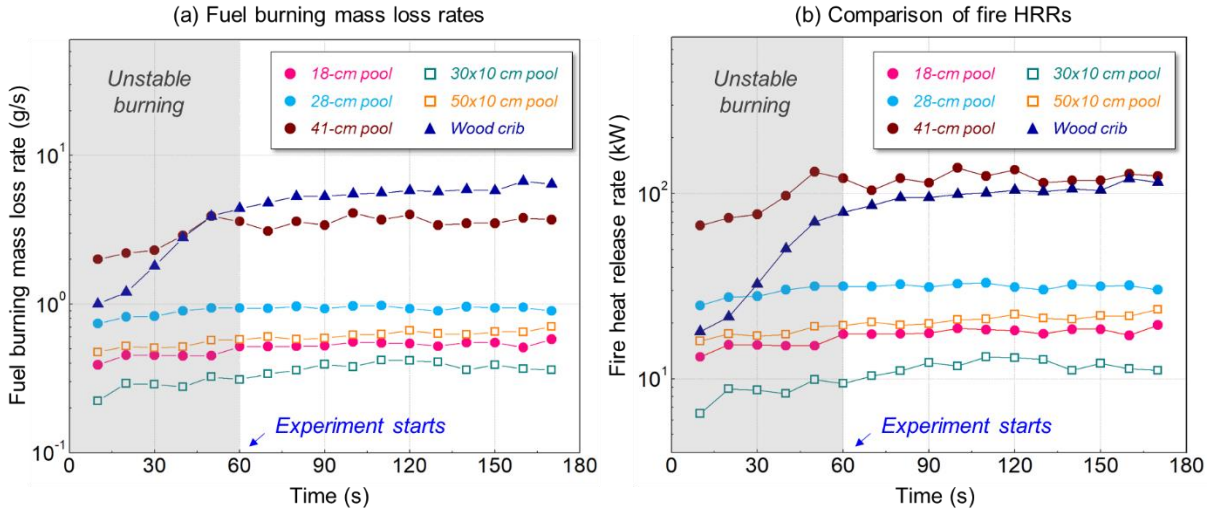

Fig. A1. The time evolution of (a) fuel mass loss rates of different fire sources and (b) the corresponding fire heat release rates (HRR).

Fig. A2a shows the background noise pressure spectra measured by the two Mics as a function of frequency. When the test room is in a quiet environment, a normal noise level around 45 dB and 30 Hz is found [39]. The noise generated by fire puffing is also quantified. For example, when the 18-cm diameter pool fire reaches a stable burning stage of 19.5 kW, two Mics mounted 0.5-m away from the fire are used to measure the fire noise spectra, see Fig. A2b. It is found that both the frequency and SPL of the fire noise are small, which are very close to the room background noise. In this way, all possible noise sources will not significantly affect the pressure-based monitoring.

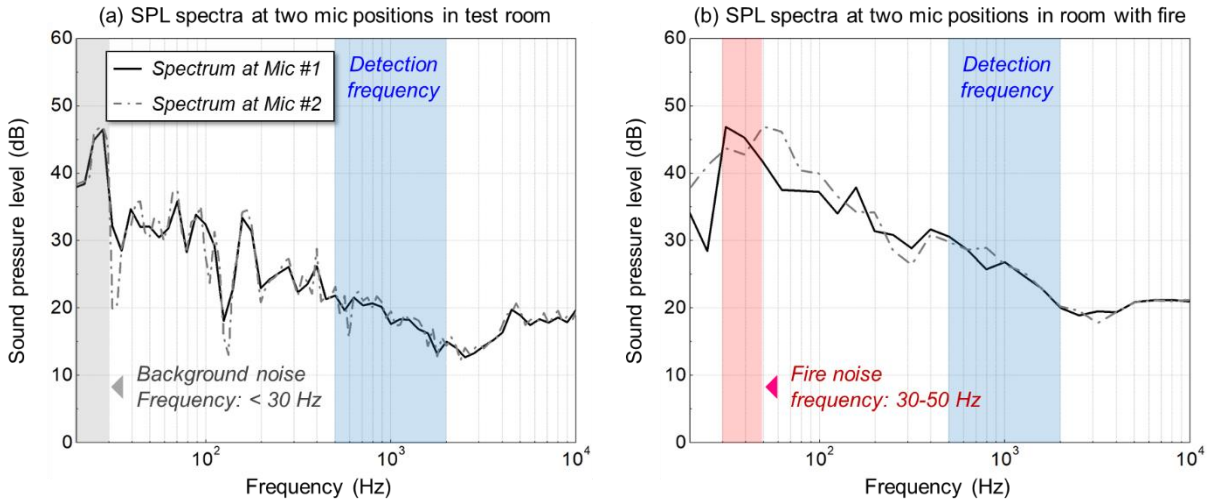

Fig. A2. Sound spectra at two Mic positions in base case for (a) room environment and (b) pool fire.